

Mode-selective thermal radiation from a microparticle

Hitoshi Odashima, Maki Tachikawa, and Kei Takehiro
Department of Physics, Meiji University, Kawasaki 214-8571, Japan
 (Received 29 April 2009; published 13 October 2009)

We experimentally demonstrate that thermal radiation from a micron-sized dielectric particle depends sensitively on its size and shape through the cavity quantum-electrodynamics effect. Our laser trapping technique levitated a high-temperature microsphere of Al_2O_3 and enabled emission spectroscopy of the single particle. As the particle becomes smaller, a blackbodylike spectrum turns into a spectrum dominated by multiple peaks resonant with whispering gallery modes of the spherical resonator. The observed sharp frequency selectivity is applicable to spectral control of thermal radiation.

DOI: [10.1103/PhysRevA.80.041806](https://doi.org/10.1103/PhysRevA.80.041806)

PACS number(s): 42.50.Wk, 44.40.+a, 42.50.Pq

Since Planck's law of blackbody radiation opened the door to quantum physics by introducing the idea of energy quantization [1,2], thermal radiation has been acknowledged as one of the most fundamental processes in nature. It plays an essential role in various physical systems spanning from cosmology [3] to atomic and molecular physics [4]. Understanding the detailed mechanism of thermal radiation is also important for practical applications such as radiation thermometry and heat transfer engineering.

A blackbody is an imaginary object defined as a perfect absorber or emitter. The spectrum of blackbody radiation is determined only by the temperature and independent of the emitter's characteristics. Thermal radiation from real objects depends on their surface asperities and chemical composition. In many cases, however, the emissivity of the surface is a moderate function of wavelength [5–7], and Planck's formula qualitatively reproduces spectral profile of the thermal radiation from macroscopic objects such as an incandescent lamp.

Recent advancement of nanotechnology has raised questions about limitations of Planck's law in microsystems or nanosystems. One of such systems is a surface-engineered macroscopic thermal emitter. Radiation properties are largely modified by surface structures with feature sizes comparable to or smaller than the characteristic wavelength of thermal radiation. Artificially fabricated periodic structures that work as photonic crystals and microcavities have been used for controlling spectral profiles, directivity, or polarization of thermal radiation [8–16]. Their potential applications include efficient light sources and sensors. These studies lead us to a more basic question about radiation properties when the emitting body itself is comparable to or smaller than the optical wavelengths. Unlike macroscopic objects, small particles should be treated as a volume emitter since not only its surface but atoms inside contribute to the thermal radiation. Theoretical analyses [17–19] have predicted morphology-dependent emission properties of dielectric microparticles; a structure, characteristic to size and shape of the particle, appears in its spectral profile since the excited material interacts mainly with radiation in the resonant optical modes inside the particle. This unique situation is realized in the intermediate particle size comparable to optical wavelengths. It is reported that thermal radiation spectra from much smaller nanoparticles well fit to Planck's formula generalized with the $1/\lambda$ emissivity correction [20–22]. The nanopar-

ticles interact with electromagnetic fields in free-space modes densely distributed over the entire frequency range and therefore retain broadband nature of the blackbody radiation like ordinary macroscopic objects.

Although examples of micron-sized objects of high temperature are found everywhere, as soot particles in combustion or sonoluminescent bubbles, clear experimental evidence of the morphology-dependent thermal radiation has not been reported. This is probably because spatial and thermal isolation of a hot single microparticle has been an experimental challenge. In this Rapid Communication, we levitate a hot microparticle of aluminum oxide (Al_2O_3) in a low pressure of air (~ 2 kPa) with our original technique of flow-assisted optical trapping [23]. The laser trap uses optical gradient force from retroreflected horizontal CO_2 laser beams [24]. Simultaneously, laminar upward convection partly cancels gravity and stabilizes the optical levitation. Data acquisition from an isolated particle provides clear relation between its size and shape and emission spectrum for direct comparison with theoretical predictions.

A microparticle of Al_2O_3 is produced by laser ablation of a coarse-grained sample with the $10\ \mu\text{m}$ radiation and then is confined in the trap. Since the lattice vibration of the particle continues to absorb the radiation from the CO_2 laser [25], it is heated to emit light as shown in the microscope charge coupled device (CCD) image of Fig. 1. The CCD image of a bright particle is likely to be larger than its actual image because of the blooming effect. By backlighting the

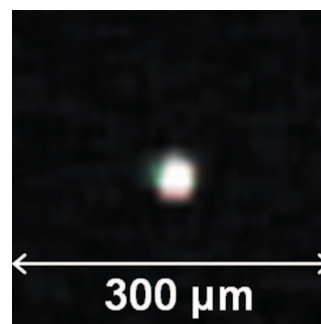


FIG. 1. (Color) Microscope image of a trapped Al_2O_3 particle. The particle stably levitates in air for minutes, absorbing the CO_2 laser radiation and emitting white light. It looks larger than its true size due to the blooming effect of the CCD.

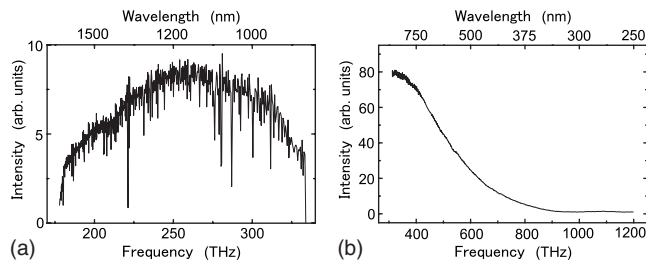


FIG. 2. Emission spectrum from a single Al_2O_3 particle. (a) Emission spectrum in the near-infrared region recorded by a multi-channel spectral analyzer with an InGaAs image sensor. Several sharp lines in the spectrum are simply due to noise in the detector. (b) Emission spectrum in the visible region recorded by a multi-channel spectral analyzer with a CCD image sensor. Unbalanced S/N ratios of the two spectra are due to the difference in the detector's sensitivity in each region.

particle and dimming the thermal emission with an interference filter, we also recorded its shadow image for accurate determination of the particle size. Trapped particles were spherical and their diameter ranged from a few to $20 \mu\text{m}$. Figure 2 shows the emission spectrum from a single microparticle in the trap recorded by calibrated multichannel spectral analyzers in the near-infrared and visible regions. The spectrum has a broadband and smooth profile with the maximum around $1.15 \mu\text{m}$, which is similar to a blackbody spectrum at a temperature of 2540 K . Since the melting point of aluminum oxide is 2327 K , the trapped microparticle would be molten. It was observed that the particle gradually got smaller due to evaporation, and the emission weakened. Figures 3(a)–3(c) show time evolution of the visible spectrum of the single particle; a series of periodic peaks appeared (a), and then each single peak separated into double peaks (b). Finally, two series of periodic peaks clearly stood out on the sloped background (c). From this moment, the emission intensity remained almost constant. A spectrum of another particle, the smallest one observed in the trap, is shown in Fig. 3(d), details of which are stated below.

To clarify the origin of the sharp resonances in the emission spectrum, we investigated a correlation of the particle size with the frequency spacing between adjacent peaks. The

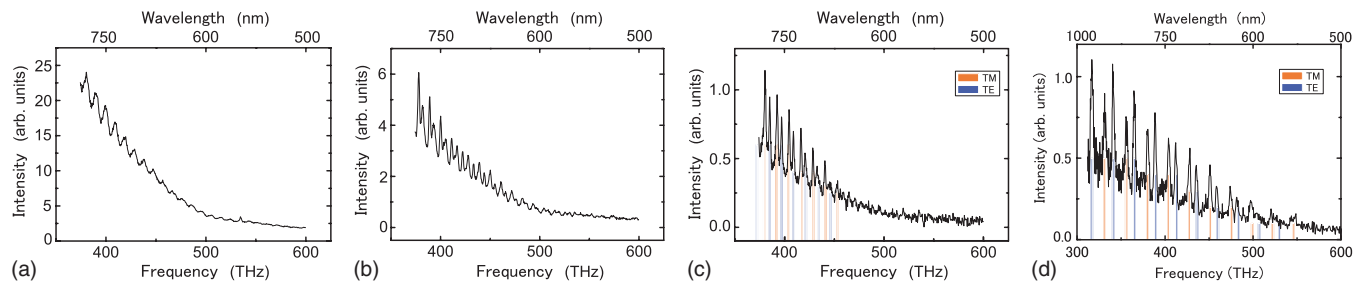


FIG. 3. (Color) Emission spectrum vs particle size. [(a)–(c)] Change in the emission spectrum as the trapped particle shrinks due to evaporation. (a) A series of periodic peaks emerges from a smooth background. The estimated particle diameter is $6.8 \mu\text{m}$. (b) Each single peak separates into double peaks when the particle size reduces to $5.8 \mu\text{m}$ by laser ablation. (c) Two series of periodic peaks are clearly resolved with a better contrast to the sloped background. The estimated particle diameter is $4.8 \mu\text{m}$. Calculated resonance frequencies of TM and TE whispering gallery modes with $q=2$ and $l=15\text{--}21$ are shown by the red and blue lines. (d) A spectrum of one of the smallest samples observed in the trap. The estimated particle diameter is $2.5 \mu\text{m}$. Calculated resonance frequencies of TM and TE whispering gallery modes with $q=1$ and $l=11\text{--}20$ are shown by the red and blue lines.

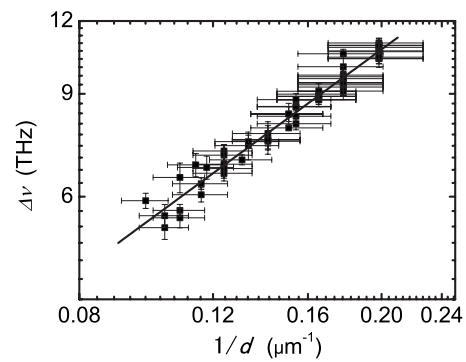


FIG. 4. Correlation between the particle diameter and the frequency spacing of the spectral peaks. The observed frequency spacing $\Delta\nu$ (THz) is plotted as a function of the inverse of the diameter d (μm). The particle diameters were determined from shadow images recorded by a digital microscope. The microscope scale was calibrated with an image of standard particles. Uncertainty in the measured diameter is due to the digitization of the shadow images. Error bars for the frequency spacing represent 1σ standard deviation. The solid line represents $\Delta\nu = Ad^{-B}$ with the best fit values of $A=50$ and $B=0.96$.

observed frequency spacing $\Delta\nu$ (THz) is plotted as a function of the inverse of the measured diameter d (μm) in Fig. 4. When two series of peaks appeared in the spectrum, we measured the frequency spacing in each series. The data for about 30 particles are fitted to $\Delta\nu = Ad^{-B}$, where A and B are adjustable parameters. The best fit values of $A = 50 \pm 3$ and $B = 0.96 \pm 0.03$ give a relation close to free spectral ranges of the whispering-gallery modes (WGMs) of a dielectric sphere [26]. The electromagnetic waves in WGMs travel around the sphere by internal reflections. WGMs of a high- Q microsphere resonator have been usefully applied in laser science and quantum optics [27–30]. WGMs in a spherical resonator are characterized by three integers l , q , and m ($|m| \leq l$) in addition to polarization TM or TE, where l is approximately the number of wavelengths in the circumference of the sphere, q is the number of radial maxima, and $l - |m| + 1$ is the number of azimuthal maxima of the field inside the sphere [30]. In a perfect sphere, modes are degenerate with respect to m . For all the modes, the free spectral ranges are approxi-

mately given by $\Delta\nu=c(\pi nd)^{-1}$, where c is the speed of light and n is the refractive index of the sphere. For aluminum oxide, $n=1.799$ [31] and one obtains $\Delta\nu=53d^{-1}$ in good agreement with the present fit. This suggests the following: a microparticle of Al_2O_3 works as a spherical cavity that modifies vacuum states of the fields and hence the rate of spontaneous emission from atoms inside depending on the degeneracy and the quality factor of the characteristic modes [32,33]. Through this cavity quantum-electrodynamics (QED) effect, thermal radiation is enhanced around frequencies resonant with the WGMs and suppressed outside their bandwidths. The TM and TE modes have a nearly equal free spectral range but have the frequency shift. The two series of periodic peaks observed in Figs. 3(b) and 3(c) are supposed to originate from the TM and TE modes.

For further verification, the accurate resonance frequencies of WGMs were obtained by solving the characteristic equations derived from the boundary condition for tangential components of electric and magnetic fields at the surface of the sphere [34]. In comparison of the calculated resonance frequencies with the observed peak frequencies, the particle diameter d , which is an adjustable parameter, was determined and the indices q and l were assigned to those modes. For the particle diameter $d=4.8\ \mu\text{m}$, the observed peaks shown in Fig. 3(c) are reproduced by the WGMs with $q=2$ and $l=15-21$; both the free spectral range and the frequency shift between TM and TE modes are in good agreement with the calculation.

We have surveyed spectra at different particle diameters from 2.5 to 12 μm and found mode series with $q=1-5$. In a considerable number of cases, the mode series characterized by a single q value dominates the whole spectrum. As the particle size decreases, the most enhanced series shifts to those of lower- q . Figure 3(d) shows a spectrum of a particle with $d=2.5\ \mu\text{m}$. This is one of the smallest particles observed in the trap. The extremely sharp resonances are due to the fundamental WGMs with $q=1$ and $l=11-20$. The spectral Q factors of those resonances are well over 100, which is in good agreement with the calculated value of ~ 130 . The Q factor is obtained from $f_r/(2f_i)$, where f_r and f_i are real and imaginary parts of the solution of the characteristic equation, respectively [34]. For molten aluminum oxide, the Q factor is limited by its fairly large extinction coefficient (7.4×10^{-3}) [31].

The size dependence of the dominant mode series is also predicted by the theoretical calculation described above. As the particle size becomes close to the wavelength, the Q factor for each mode starts to decrease and more energy leaks out of the sphere. Eventually, that mode fades away when the cut-off frequency exceeds its resonance frequency. The mode series with a larger index q approaches the cut-off frequency at a larger particle size and resonant peaks successively disappear. As shown in Fig. 3, the emission spectrum has higher peak contrast as the particle becomes smaller; each peak is better resolved with a less background. This is explained by disappearance of higher- q modes and expansion of the free spectral range. Resonant peaks sharpen for a smaller particle possibly because an increased surface tension changes the molten particle into a more ideal sphere, and modes become more degenerate with respect to the index m [30].

In summary, we have observed an emission spectrum of a single high-temperature Al_2O_3 particle and clearly demonstrated a transition from a blackbody-type thermal radiation to a mode-selective thermal radiation with a decrease in the particle size. The regular structures in the emission spectrum are due to the resonances with the whispering gallery modes characteristic to the spherical resonator. The present experiment suggests that suppression and enhancement of the thermal radiation via the cavity QED effect is generally observable in natural dielectric bodies if the dimension is comparable to the wavelength of interest. Carefully arranged experiments will verify this effect in other physical systems. From a practical view point, morphology of the microparticles provides a knob to control the thermal emission properties. Several groups [8–11] realized resonant enhancement of specific wavelengths through excitation of characteristic modes in the microcavities artificially fabricated on W or Si surfaces. Compared with their results, dielectric microparticles are attractive since (i) their resonances on WGMs are an order of magnitude sharper than those of open cavities, (ii) the spectral control is available also in the visible region, and (iii) mode structures are controllable by choosing the size and shape of the particle.

We thank K. Nakagawa for discussions on emission spectroscopy and T. Kitazaki, R. Kukimiya, and S. Shimizugawa for assistance with the experiment.

-
- [1] M. Planck, Verh. Dtsch. Phys. Ges. **2**, 202 (1900).
 [2] M. Planck, Verh. Dtsch. Phys. Ges. **2**, 237 (1900).
 [3] A. A. Penzias and R. W. Wilson, Astrophys. J. **142**, 419 (1965).
 [4] A. Einstein, Phys. Z. **18**, 121 (1917).
 [5] M. Q. Brewster, *Thermal Radiative Transfer and Properties* (Wiley, New York, 1992).
 [6] R. D. Larrabee, J. Opt. Soc. Am. **49**, 619 (1959).
 [7] E. Takasuka, E. Tokizaki, K. Terashima, and S. Kimura, Appl. Phys. Lett. **67**, 152 (1995).
 [8] P. J. Hesketh, J. N. Zemel, and B. Gebhart, Nature (London) **324**, 549 (1986).
 [9] S. Maruyama, T. Kashiwa, H. Yugami, and M. Esashi, Appl. Phys. Lett. **79**, 1393 (2001).
 [10] H. Sai, Y. Kanamori, and H. Yugami, Appl. Phys. Lett. **82**, 1685 (2003).
 [11] F. Kusunoki, T. Kohama, T. Hiroshima, S. Fukumoto, J. Takahara, and T. Kobayashi, Jpn. J. Appl. Phys. **43**, 5253 (2004).
 [12] J.-J. Greffet, R. Carminati, K. Joulain, J.-P. Mulet, S. Mainguy, and Y. Chen, Nature (London) **416**, 61 (2002).
 [13] I. Celanovic, D. Perreault, and J. Kassakian, Phys. Rev. B **72**, 075127 (2005).

- [14] M. U. Pralle, N. Moelders, M. P. McNeal, I. Puscasu, A. C. Greenwald, J. T. Daly, E. A. Johnson, T. George, D. S. Choi, I. El-Kady, and R. Biswas, *Appl. Phys. Lett.* **81**, 4685 (2002).
- [15] S.-Y. Lin, J. G. Fleming, and I. El-Kady, *Opt. Lett.* **28**, 1909 (2003).
- [16] S.-Y. Lin, J. G. Fleming, E. Chow, J. Bur, K. K. Choi, and A. Goldberg, *Phys. Rev. B* **62**, R2243 (2000).
- [17] S. C. Ching, H. M. Lai, and K. Young, *J. Opt. Soc. Am. B* **4**, 1995 (1987).
- [18] S. Lange and G. Schweiger, *J. Opt. Soc. Am. B* **11**, 2444 (1994).
- [19] A. M. García-García, *Phys. Rev. A* **78**, 023806 (2008).
- [20] E. Rohlfing, *J. Chem. Phys.* **89**, 6103 (1988).
- [21] R. Mitzner and E. B. Campbell, *J. Chem. Phys.* **103**, 2445 (1995).
- [22] K. Elihn, L. Landström, and P. Heszler, *Appl. Surf. Sci.* **186**, 573 (2002).
- [23] T. Ochiai, M. Numoto, M. Tachikawa, and H. Odashima, *Jpn. J. Appl. Phys.* **46**, L957 (2007).
- [24] S. Friebel, C. D'Andrea, J. Walz, M. Weitz, and T. W. Hänsch, *Phys. Rev. A* **57**, R20 (1998).
- [25] C. H. Shek and J. K. L. Lai, *Nanostruct. Mater.* **8**, 605 (1997).
- [26] S. Schiller and R. L. Byer, *Opt. Lett.* **16**, 1138 (1991).
- [27] V. R. Braginsky, M. L. Gorodetsky, and V. S. Ilchenko, *Phys. Lett. A* **137**, 393 (1989).
- [28] M. Kuwata-Gonokami and K. Takeda, *Opt. Mater. (Amsterdam, Neth.)* **9**, 12 (1998).
- [29] D. W. Vernooy, A. Furusawa, N. Ph. Georgiades, V. S. Ilchenko, and H. J. Kimble, *Phys. Rev. A* **57**, R2293 (1998).
- [30] V. V. Vassiliev, V. L. Velichansky, V. S. Ilchenko, M. Gorodetsky, L. Hollberg, and A. V. Yarovitsky, *Opt. Commun.* **158**, 305 (1998).
- [31] J. M. A. Adams, *J. Quant. Spectrosc. Radiat. Transf.* **7**, 273 (1967).
- [32] D. Kleppner, *Phys. Rev. Lett.* **47**, 233 (1981).
- [33] Y. Z. Wang, B. L. Lu, Y. Q. Li, and Y. S. Liu, *Opt. Lett.* **20**, 770 (1995).
- [34] J. A. Stratton, *Electromagnetic Theory* (McGraw-Hill, New York, 1941).